SciEn
Journal of Engineering Advancements Vol. 05(01) 2024, pp 14-18 https://doi.org/10.38032/jea.2024.01.003

Heat Transfer Mechanism over a Trapezium-Shaped Device Including Heat Conductive Solid Circular Metal Block

M. U. Ahammad, Abdur Rahim, Abu Hanifa

Department of Mathematics, Dhaka University of Engineering and Technology, Gazipur-1707, Bangladesh

Received: November 26, 2023, Revised: February 08, 2024, Accepted: February 08, 2024, Available Online: March 10, 2024

ABSTRACT

Combined convective flow design and heat transfer efficiency are investigated in this research for variation of some pertinent parameters inside a trapezoidal device along with heat conductive solid circular block. By the implementation of the Finite element method, flow, and heat transfer behavior are presented in detail for the ranges of Reynolds number, $50 \leq Re \leq 200$, and Hartmann number, $20 \leq Ha \leq 150$ along with mixed convection parameter $Ri = 1$. Obtained results for the flow and temperature field in the considered domain are shown in terms of the streamlines and isotherms. In addition, the heat transfer rate at the bottom heated and ceiling cold wall is presented by $Nu_{av.}$ A noteworthy heat transfer augmentation is found at both heated and cold surfaces due to upper values of Re. Interestingly, the better cooling efficiency of the device is marked out for the hot wall.

Keywords: Heat Transfer, Trapezoidal Device, Heat Conduction, Solid Metal Block.

Copyright @ All authors

This work is licensed under a Creative Commons Attribution-Non Commercial 4.0 International License.

1 Introduction

Free and forced convection is a crucial issue in fluid flow and thermal systems of different geometrical configurations. Due to the many engineering and industrial applications, such types of phenomena have received great concentration from researchers and are frequently encountered in cooling systems for electronic equipment, thermal insulation, energy storage, and heat exchangers.

Mamun *et al.* [1] analyzed mixed convection analysis in the trapezoidal cavity with a moving lid. Two-dimensional MHD free convection with internal heating in a square cavity was presented by Taghikhani and Chavoshi [2]. Mixed convection enhancement in a rectangular cavity by triangular obstacle was presented by Afluq *et al.* [3]. Ibrahim and Hirpho [4] carried out combined convection flow in a trapezoidal domain taking non-uniform temperature. Abdul Halim Bhuiyan *et al.* [5] studied the effect of the Hartmann Number on free convective flow in a square cavity with different positions of heated square block. Shuja *et al.* [6] performed a heat-generating rectangular body effect of cavity exit port locations in a square enclosure. Mixed convection from an isolated heat source in a rectangular enclosure was performed by Papanicolaou and Jaluria [7]. Raji and Hasnaoui *et al.* [8] presented mixed convection heat transfer in a rectangular cavity ventilated and heated from the side. An experimental investigation of combined convection in a channel with a vented cavity was carried out by Manca *et al.* [9]. Analysis of free convection around a square heated cylinder kept in a cavity was explained by Kumar and Dalal [10]. Rahman *et al.* [11] performed mixed convection in a vented square cavity with a heat-conducting horizontal solid circular cylinder. Gau *et al.* [12] investigated an experimental study on mixed convection in a horizontal rectangular channel heated from a side. Sheremet *et al.* [13] studied natural convective heat transfer through two entrapped triangular cavities filled with a nanofluid. Brown *et al.* [14] studied mixed convection from an open cavity in a horizontal channel.

From the literature cited above and according to the authors' knowledge, it is followed that no work has been performed yet for the specified configuration of the current problem. The goal of the present research is to investigate combined convection flow and heat transfer behavior in a trapezoidal-shaped domain having a heat conductive circular block for the variation of Reynolds and Hartmann number.

2 Geometry and Mathematical Model

The considered domain of this problem is depicted in Fig. 1, which is formed by a trapezoidal enclosure whose lower and upper sides are of the length $2L$ and $L/2$ respectively. A heat-conductive circular block is placed at the center of the cavity. The bottom surface is heated and the top surface is cooled accordingly as $T_h > T_c$. The two inclined walls of the domain are considered adiabatic. A uniform magnetic field of strength B_0 is applied to the flat direction of the left wall.

In the current study, the working fluid is considered as 2-D steady, laminar, and Newtonian with constant thermo-physical properties. The leading equations for the problem in non-dimensional form are given below:

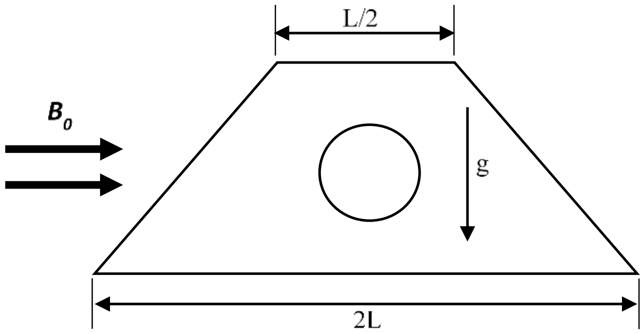

Fig. 1 Schematic sketch of the problem

*Corresponding Author Email Address: mainuddin633@duet.ac.bd Published by: SciEn Publishing Group

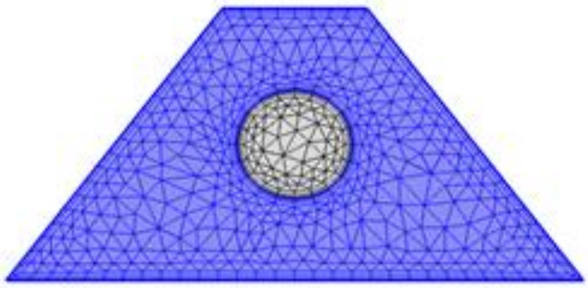

Fig. 2 Typical Grid generation

$$\frac{\partial U}{\partial X}+\frac{\partial V}{\partial Y}=0 \tag{1}$$

$$U\frac{\partial U}{\partial X}+V\frac{\partial U}{\partial Y}=-\frac{\partial P}{\partial X}+\frac{1}{Re}\left(\frac{\partial^2 U}{\partial X^2}+\frac{\partial^2 U}{\partial Y^2}\right) \tag{2}$$

$$U\frac{\partial V}{\partial X}+V\frac{\partial V}{\partial Y}=-\frac{\partial P}{\partial X}+\frac{1}{Re}\left(\frac{\partial^2 V}{\partial X^2}+\frac{\partial^2 V}{\partial Y^2}\right)+Ri\theta-\frac{Ha^2}{Re}V \tag{3}$$

$$U\frac{\partial \theta}{\partial X}+V\frac{\partial \theta}{\partial Y}=\frac{1}{RePr}\left(\frac{\partial^2 \theta}{\partial X^2}+\frac{\partial^2 \theta}{\partial Y^2}\right) \tag{4}$$

For heat-conducting circular body,

$$\frac{K}{RePr}\left(\frac{\partial^2 \theta_s}{\partial X^2}+\frac{\partial^2 \theta_s}{\partial Y^2}\right) \tag{5}$$

The following non-dimensional variables are used in order to obtain the above dimensionless governing Eqs. (1)–(5), $X=\frac{x}{L},\ Y=\frac{Y}{L},\ U=\frac{u}{u_i}, V=\frac{v}{u_i}, P=\frac{p}{\rho u_i^2},\ \theta=\frac{(T-T_C)}{(T_h-T_C)},\ \theta_s=\frac{(T_s-T_c)}{(T_h-T_c)}$

Where X and Y are the coordinates varying along horizontal and vertical directions; U, and V are the velocity components in the X and Y directions respectively. Also θ and θ_s are the dimensionless temperature of fluid and solid respectively and P is the dimensionless pressure.

The governing parameters are defined correspondingly as

$$Re=\frac{u_i L}{v},\ Pr=\frac{v}{\alpha},\ Ha=B_0 L\sqrt{\frac{\sigma}{\mu}},\ Ri=\frac{Gr}{Re^2}$$

($u_i$is the reference velocity of fluid and B0 is magnetic field strength)

The imposed boundary conditions are as follows:

At upper surface: $U=0, V=0, \theta=0$; at lower surface: $U=0, V=0, \theta=1$; and at two side walls: $U=0, V=0, \frac{\partial\theta}{\partial N}=0$

Also, Nu_{av} at the heated wall is calculated using $Nu_{av}=-\int_0^1\left(\frac{\partial\theta}{\partial Y}\right)dX$

3 Grid Refinement Test and Validity of the Code

Various grid-sized elements are taken to find the optimum accurateness of the result for the considered problem. A typical grid size distribution is shown in Fig. 2. The heat transfer rate at the bottom wall of the cavity is calculated for the selected grids. A slight difference is noticed among the results for the variation of grid size which is tabulated in Table 1. Finally, the grid containing 2184 elements is taken into account for computing Nu_{av} at the hot wall. Table 2 shows the thermo-physical properties of water and aluminum used in this work.

Table 1 Nu_{av} at bottom surface for Pr = 7.1, Re = 100, Ha = 20, Ri = 1

No. of elements	621	886	1456	2184	3384
Nu_{av}	6.9638	6.9062	6.8694	6.8677	6.8662
Deviation	-	0.0576	0.0368	0.0017	0.0015

Table 2 Thermo physical properties of water and aluminum

Property	Water	Aluminum (Al)
$C_p\ (Jkg^{-1}K^{-1})$	4179	902
$\rho\ (kgm^{-3})$	997.1	2701
$k\ (Wm^{-1}K^{-1})$	0.613	237
$\beta\ (K^{-1})$	21×10^{-5}	23.1×10^{-6}
$\sigma\ (S/m)$	.05	3.5×10^{7}

For the code validation of the present work, a computation is performed for comparison with the previously published work that was performed by the authors Ibrahim and Hirpho [4]. Fig. 3 exposes the relationship between these two works with a good agreement in velocity and temperature fields that are demonstrated as streamlines and isotherms.

4 Results and Discussions

In this work, two-dimensional steady flow and thermal field are investigated to test the effect of Re and Ha inside the studied configuration. The streamlines, isotherms, and average Nusselt number are exhibited to clarify the flow and temperature ground of the problem for the range of Hartmann number 20 ≤ Ha ≤ 150 along with mixed convection parameter Ri = 1 and Prandtl number Pr = 7.1.

Reynolds number's effect on velocity and temperature profile in the range of 50 to 200 is displayed in Fig. 4. Fig. 4 (a) exposes that at low Reynolds number Re = 50, large-sized vortexes are created surrounding the centered circular block. For the next higher values Re = 100 and Re = 150, the flow patterns are all most similar. But for the largest value of Re = 200, the intensity of the left-sided vortex increases consequently vorticity of the right-sided vortex reduces.

In Fig. 4 (b), the isotherms for different Reynolds numbers are exposed and this figure shows that heat lines are non-linear occupying the total region and dense in the neighborhood of the top cooled wall at Re = 50. Also, the centered body is encircled by the thermal lines and comparatively more heated lines are found near the heated lower surface. No visible alteration is tracked for the three rising values of Re = 100, 150, 200.

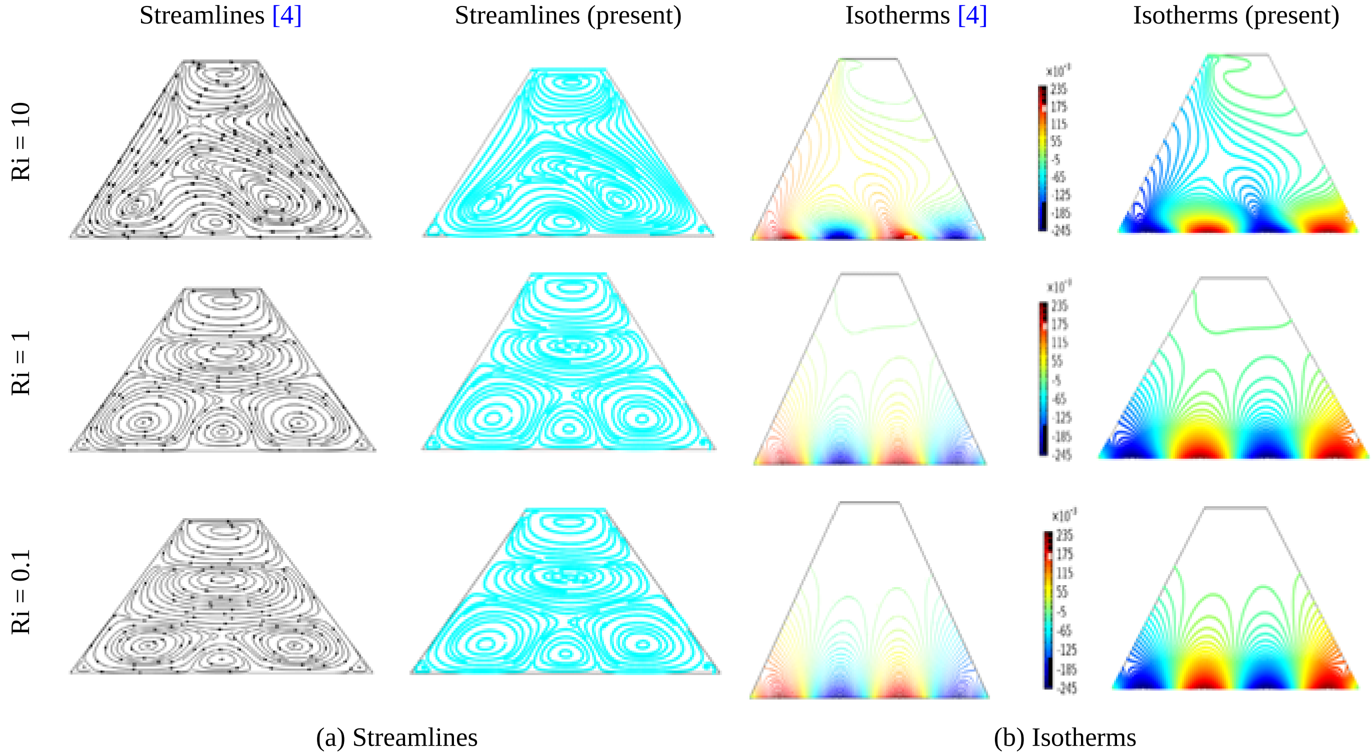

Fig. 3 Relationship between the present and the work of Ibrahim and Hirpho [4] at Gr = 10^4, Pr = 6.2, Ha = 50, and Re = 100

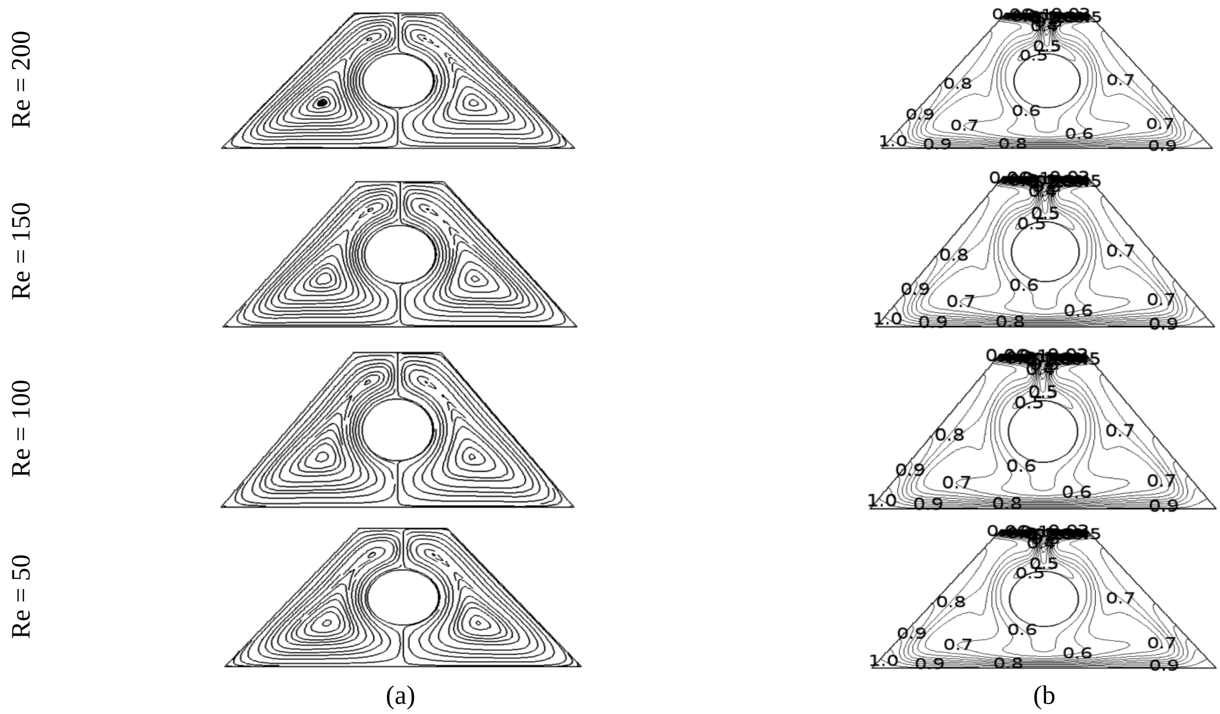

Fig. 4 (a) Streamlines and (b) Isotherms for variation of Re at Pr =7.1, Ri = 1, Ha = 20

In Fig. 5, streamlines and isotherms are exhibited for the various values of Ha that vary from 20 to 150. One can observe from Fig. 5(a) that at low Hartmann number Ha = 20 the streamlines captured the whole cavity by the about two symmetric vortices concerning the interior body. A minor discrepancy is noticed for Ha = 50. For the mounting values of Ha = 100 and Ha = 150 a significant change is noticed, the vortex strength increases near the bottom and top surface, especially for Ha = 150.

The corresponding thermal lines distributions in the enclosure for different Hartmann numbers are illustrated in Fig. 5 (b). With a small change the heat lines are found non-uniform that are elongated from the left side to the right side of the cavity for Ha = 20 and Ha = 50. A thick boundary layer is created at the top wall. In addition, heat lines are comparatively linear and symmetric about the circular body for the two larger values of Ha = 100 and Ha = 150. More heated heat lines are located at the bottom part of the enclosure; thermal lines are concentrated above the circular block.

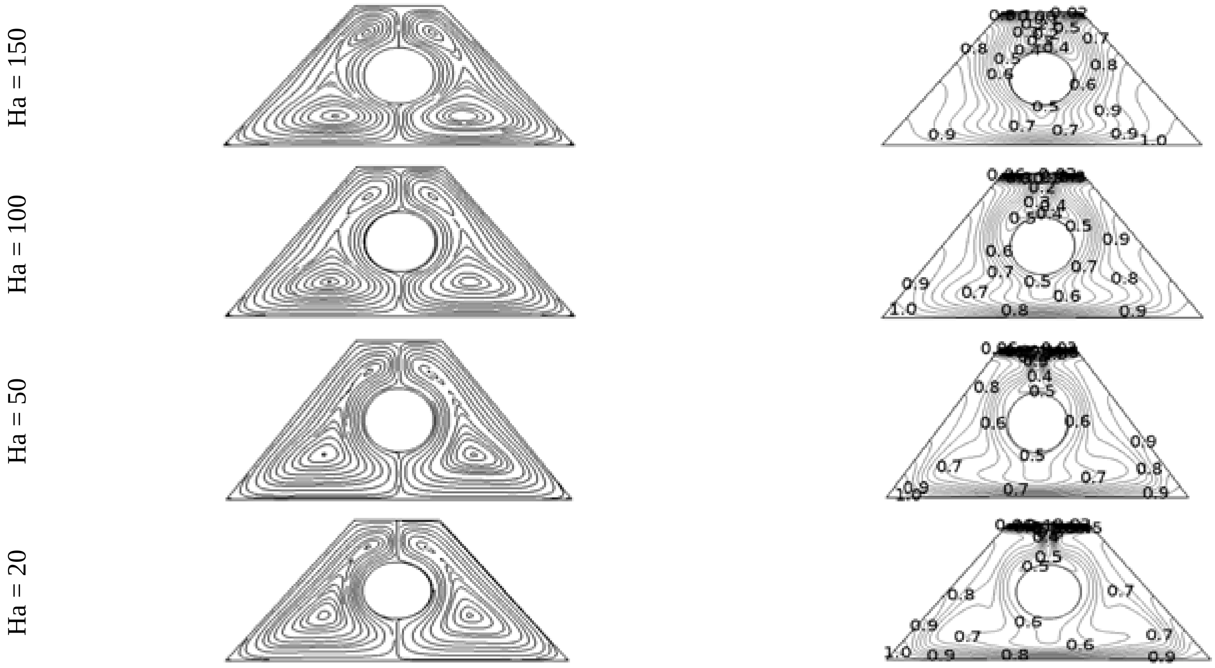

(a) (b)

Fig. 5 (a) Streamlines and (b) Isotherms for different values of Ha at Pr =7.1, Ri = 1, Re =100

Fig. 6 shows the average Nusselt number at both heated and cold wall for the variation of (a) Reynolds number and (b) Hartmann number. This figure reveals that higher heat removal is obtained for the upper values of Reynolds number while Nu_{av} reduces for the higher values of Ha due to its resistance.

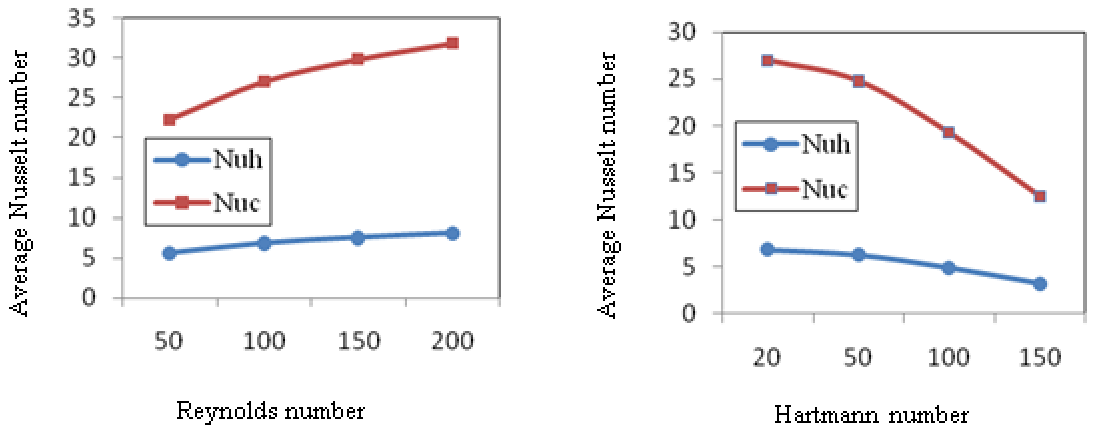

Fig. 6 Heat transfer rate at ceiling and ground walls for different values of (a) Reynolds number and (b) Hartmann number

The rate of heat transfer at bottom heated and top cooled walls for chosen values of Reynolds number are shown in Table 3. From the table, it can be followed that the heat removal rate at hot and cool walls increases with the mounting values of Re and vice versa.

Table 3 Average Nusselt number for variation of Re while Pr = 7.1, Ha = 20 and Ri = 1

Re	***$(Nu_{av})_{hot}$***	***$(Nu_{av})_{cool}$***
50	5.6635	22.206
100	6.8677	26.980
150	7.5679	29.765
200	8.0859	31.806

Nu_{av} at ground and ceiling surfaces for different values of Ha that are listed in Table 4 and it is noticed that cooling efficiency at both walls enhances the smaller values of Ha.

Table 4 Average Nusselt number for variation of Ha while Pr = 7.1, Re = 100 and Ri = 1

Ha	***$(Nu_{av})_{hot}$***	***$(Nu_{av})_{R\ cool}$***
20	6.8677	26.980
50	6.3227	24.804
100	4.9307	19.279
150	3.2079	12.496

5 Conclusions

The influence of Re and Ha along with Ri on flow and thermal field have been analyzed in a trapezoidal domain with an internal heat conductive circular body. The obtained results of the problem are stated concisely below:

- Significant improvement in heat transfer is recorded at both hot and cold walls due to higher values of Re, consequently smaller value of Reynolds number gives the lowest heat removal.
- As Ha increases, Nu_{av} decreases at the heated and cold surface, so optimum heat transfer is found for the lowest Hartmann number.
- Comparatively rapid change in heat removal is followed at the bottom heated wall.

References

[1] Mamun, M.A.H., Tanim, T.R., Rahman, M.M., Saidur, R. and Nagata, S., 2010. Mixed convection analysis in trapezoidal cavity with a moving lid. International Journal of Mechanical and Materials Engineering, 5(1), pp.18-28.

[2] Taghikhani, M.A. and Chavoshi, H.R., 2013. Two dimensional MHD free convection with internal heating in a square cavity. Thermal Energy and Power Engineering, 2(1), pp.22-28.

[3] Afluq, S.G., Siba, M.A.A.A. and Jehhef, K.A., 2020, July. Mixed convection enhancement in a rectangular cavity by triangular obstacle. In IOP Conference Series: Materials Science and Engineering (Vol. 881, No. 1, p. 012083). IOP Publishing.

[4] Ibrahim, W. and Hirpho, M., 2021. Finite element analysis of mixed convection flow in a trapezoidal cavity with non-uniform temperature. Heliyon, 7(1).

[5] Bhuiyan, A.H., Alim, M.A. and Uddin, M.N., 2014. Effect of Hartmann number on free convective flow in a square cavity with different positions of heated square block. International Journal of Physical and Mathematical Sciences, 8(2), pp.385-390.

[6] Obayedullah, M., Chowdhury, M.M.K. and Rahman, M.M., 2013. Natural convection in a rectangular cavity having internal energy sources and electrically conducting fluid with sinusoidal temperature at the bottom wall. International Journal of Mechanical and Materials Engineering, 8(1), pp.73-78.

[7] Papanicolaou, E. and Jaluria, Y., 1991. Mixed convection from an isolated heat source in a rectangular enclosure. Numerical Heat Transfer, 18(4), pp.427-461.

[8] Raji, A. and Hasnaoui, M., 1998. Mixed convection heat transfer in a rectangular cavity ventilated and heated from the side. Numerical Heat Transfer, Part A Applications, 33(5), pp.533-548.

[9] Manca, O., Nardini, S. and Vafai, K., 2006. Experimental investigation of mixed convection in a channel with an open cavity. Experimental heat transfer, 19(1), pp.53-68.

[10] De, A.K. and Dalal, A., 2006. A numerical study of natural convection around a square, horizontal, heated cylinder placed in an enclosure. International journal of heat and mass transfer, 49(23-24), pp.4608-4623.

[11] Rahman, M., Alim, M.A., Saha, S. and Chowdhury, M.K., 2008. Mixed convection in a vented square cavity with a heat conducting horizontal solid circular cylinder. Journal of naval architecture and marine engineering, 5(2), pp.37-46.

[12] Gau, C., Jeng, Y.C. and Liu, C.G., 2000. An experimental study on mixed convection in a horizontal rectangular channel heated from a side. J. Heat Transfer, 122(4), pp.701-707.

[13] Sheremet, M.A., Revnic, C. and Pop, I., 2017. Natural convective heat transfer through two entrapped triangular cavities filled with a nanofluid: Buongiorno's mathematical model. International journal of mechanical sciences, 133, pp.484-494.

[14] Leong, J.C., Brown, N.M. and Lai, F.C., 2005. Mixed convection from an open cavity in a horizontal channel. International Communications in Heat and Mass Transfer, 32(5), pp.583-592.